Organic & Biomolecular Chemistry

RSC Publishing

PAPER

View Article Online
View Journal | View Issue

Cite this: *Org. Biomol. Chem.*, 2013, **11**, 1326

A rotaxane host system containing integrated triazole C–H hydrogen bond donors for anion recognition†

Nicholas G. White and Paul D. Beer*

Received 16th November 2012,
Accepted 18th December 2012

DOI: 10.1039/c2ob27229f

www.rsc.org/obc

Two rotaxanes incorporating a 3,5-bis(triazole)-pyridinium axle component have been prepared using either an anion templated amide condensation or ring closing metathesis (RCM) clipping strategy. The respective yields of interlocked receptor were found to be significantly higher when the RCM clipping synthetic route was used. Proton NMR titration experiments in competitive 1 : 1 $CDCl_3$–CD_3OD solvent media reveal that the rotaxane prepared by the clipping procedure is selective for halide anions over larger, more basic oxoanions. Interestingly, the interlocked host displays an unusual preference for bromide over other halide anions.

Introduction

Since independent reports in 2008 demonstrated that synthetic host systems containing 1,2,3-triazole groups can interact with anions in organic solvents solely through C–H···anion hydrogen bonds,[1–3] numerous receptors incorporating these heterocycles have been described.[4–28] These triazole groups can be readily prepared using copper(I)-catalyzed azide–alkyne cycloaddition (CuAAC) reactions,[29,30] and indeed this reaction has frequently been used to construct mechanically interlocked architectures.[31–35] Surprisingly, however, to the best of our knowledge, only two[36] triazole containing interlocked host systems have been reported where the triazole group is used as an anion recognition motif.[37,38]

Li and co-workers' triazole axle containing rotaxane acts as a dual response molecular switch, with translocation of the macrocyclic component occurring in response to acid/base stimulus, and chloride anion addition causing subsequent rotation of the macrocycle.[37] Furthermore, the non-protonated form of the rotaxane was reported to display modest association with halide anions in CD_3CN.

We recently reported a catenane containing a 3,5-bis(triazole)-pyridinium motif (Fig. 1), which selectively binds halide anions over dihydrogenphosphate in competitive 1 : 1 $CDCl_3$–CD_3OD solvent mixtures.[38] Importantly, this selectivity is an order of magnitude more pronounced for the triazole containing host than for the analogous 3,5-bis(amide)-pyridinium catenane receptor.

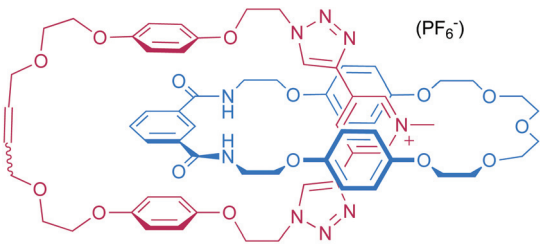

1·PF$_6$

Fig. 1 Halide anion selective bis-triazole pyridinium catenane **1·PF$_6$**.[38]

Previous rotaxane receptor systems have displayed stronger and more selective anion recognition when compared to catenane analogues. This was attributed to their more rigid structure, and the introduction of aryl–axle substituents to the amide donor groups, increasing the acidity of these hydrogen bond donors.[39] Herein, we describe the integration of the bis-triazole pyridinium motif into the axle component of a rotaxane structural framework and investigate the anion recognition properties of the resulting interlocked host.

Results and discussion

Two chloride anion templated synthetic procedures were undertaken to prepare the target triazole containing rotaxane host structure, an acid chloride/amine condensation reaction[40] and a RCM clipping protocol.[41] Both synthetic routes required the initial preparation of a new 3,5-bis(triazole)-pyridinium axle component.

Chemistry Research Laboratory, Department of Chemistry, University of Oxford, 12 Mansfield Road, Oxford, OX1 3TA, UK. E-mail: paul.beer@chem.ox.ac.uk; Fax: +44 (0) 1865 272690; Tel: +44 (0) 1865 285142

†Electronic supplementary information (ESI) available: ^1H and ^{13}C NMR spectra of new compounds, ROESY NMR spectrum of **9·PF$_6$**, details of instrumentation, titration protocols and full crystallographic data in CIF format. CCDC 911205 and 911206. For ESI and crystallographic data in CIF or other electronic format see DOI: 10.1039/c2ob27229f

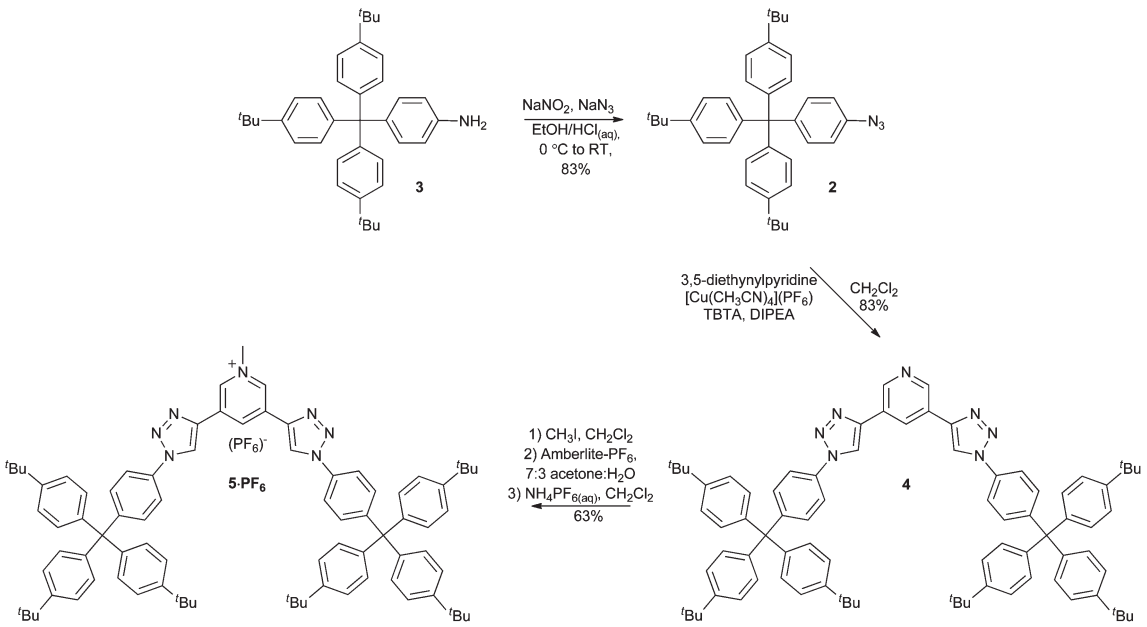

Scheme 1 Synthesis of axle component **5·PF$_6$**.

Synthesis of bis-triazole pyridinium axle component

The azide-appended stopper group **2** was prepared from amine **3**[42] using sodium nitrite and sodium azide in 9 : 1 ethanol–conc. $HCl_{(aq)}$ (Scheme 1). CuAAC reaction of two equivalents of **2** and 3,5-diethynyl pyridine[43] gave the bis-triazole axle component **4** in 83% yield. Selective alkylation of the pyridine group was achieved using excess methyl iodide in dichloromethane at room temperature to give **5·I**. It was found that halide salts of 5^+ exhibited very poor solubility in common organic solvents, and as a consequence **5·I** was anion exchanged using Amberlite® resin to give **5·PF$_6$** in an overall yield of 63% from **4**.

Synthesis of rotaxane *via* amide condensation strategy

Rotaxane formation was initially attempted *via* condensation of a bis-amine and bis-acid chloride in the presence of axle component 5^+, as this synthetic procedure has proven to be an effective method for preparing rotaxanes containing a bis-amide pyridinium axle component.[40,44] An equimolar mixture of axle **5·PF$_6$**,[45] bis-amine **6**[46] and isophthaloyl dichloride were stirred in dry dichloromethane containing excess triethylamine (Scheme 2). Integration of the ^{1}H NMR spectrum of the crude reaction mixture indicated that the rotaxane had formed in approximately 20% yield. After purification by preparative TLC and anion exchange by washing the product with aqueous NH_4PF_6, the target rotaxane **7·PF$_6$** was isolated in 11% yield, and characterized by ^{1}H and ^{19}F NMR spectroscopy, as well as high resolution ESI mass spectrometry. Twinned crystals of **7·PF$_6$** suitable for X-ray diffraction structural analysis were obtained, enabling solid state characterization and confirmation of the interlocked nature of the product (Fig. 2). Three weak rotaxane···PF_6^- hydrogen bonds are observed, two from the axle component's triazole donors and one from a macrocycle amide group. Surprisingly no aromatic donor–acceptor interactions are observed between the pyridinium ring of the axle and the macrocycle's hydroquinone groups (closest centroid···centroid distance = 3.99 Å).

Synthesis of rotaxane *via* clipping

Given the small amounts of rotaxane isolated using an amide condensation route, a clipping strategy[41] was instead investigated for the preparation of the target triazole containing rotaxane (Scheme 3). The addition of Grubbs' II catalyst to an 1 : 1 : 1.5 stoichiometric mixture of **5·PF$_6$**, TBA·Cl (TBA = tetrabutylammonium) and bis-vinyl-appended macrocycle precursor **8**[47] in dry dichloromethane gave the target rotaxane 9^+, with integration of the crude ^{1}H NMR spectrum indicating a yield of formation of approximately 65%.

Purification by preparative TLC, anion exchange by washing with $NH_4PF_{6(aq)}$ and recrystallisation afforded **9·PF$_6$** in 44% overall isolated yield. The new rotaxane was characterized by ^{1}H, ^{13}C, ^{19}F and ^{31}P NMR, as well as by high resolution ESI mass spectrometry. The interlocked nature of the rotaxane was also confirmed by 2D ROESY NMR spectroscopy (Fig. S10†).

The synthesis of analogous rotaxanes containing a bis-amide pyridinium axle component proceeded in similar yields *via* RCM clipping (43–57%)[41,47] or amide condensation (55–60%) strategies.[40] By contrast, with the bis-triazole pyridinium axle component **5·PF$_6$**, the crude and isolated yields of rotaxane are significantly higher for clipping than condensation (65 and 20% crude yields, and 44 and 11% isolated yields for clipping and condensation, respectively).

Anion recognition properties of 9·PF$_6$

The anion recognition properties of **9·PF$_6$** were investigated using ^{1}H NMR titration experiments in the competitive solvent

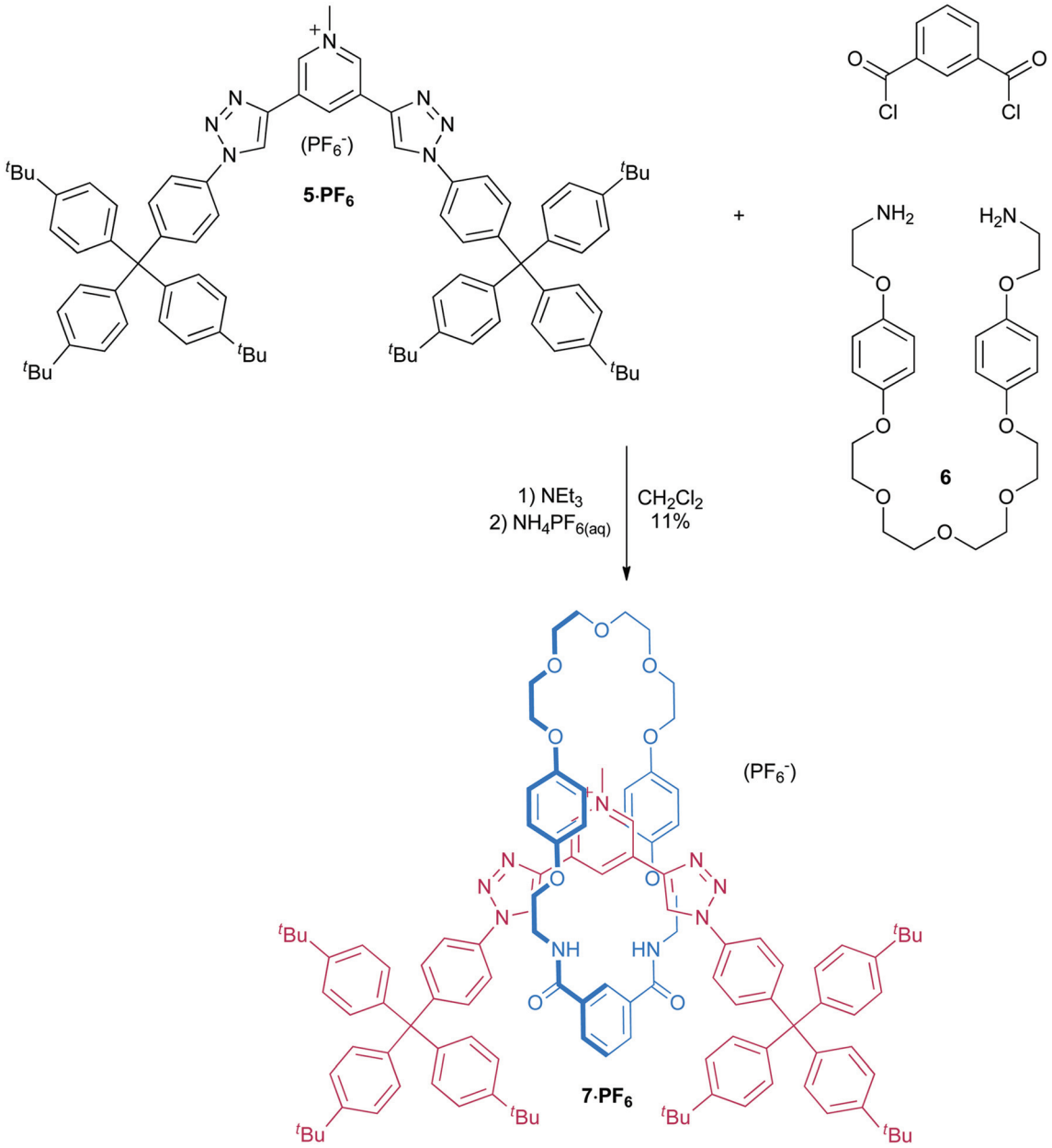

Scheme 2 Synthesis of rotaxane **7·PF$_6$**.

mixture 1 : 1 $CDCl_3$–CD_3OD. Addition of halide anions to **9·PF$_6$** causes downfield shifts in the rotaxane's cavity resonances a–c and 1–3 (Fig. 3), consistent with hydrogen bonding between these protons and the anion. Interestingly, the addition of chloride and bromide anions to **9·PF$_6$** causes significantly smaller shifts in the cavity protons than was observed for the analogous bis-triazole pyridinium catenane **1·PF$_6$**.[38] Given its lower basicity compared to chloride and bromide, it is noteworthy that iodide causes the largest magnitude perturbations (Fig. 4).

WINEQNMR2[48] analysis of the titration data, monitoring the axle component's triazole resonance determined 1 : 1 stoichiometric association constants (Table 1), which are compared with association constant values obtained for the bis-triazole pyridinium catenane **1·PF$_6$**.[38] The rotaxane host displays an unusual preference for bromide anion, with this halide being bound significantly more strongly than iodide, which is itself complexed more strongly than chloride. This may be a result of the complementary size of the axle's 3,5-bis(triazole)-pyridinium binding cleft, which is two atoms larger than in the analogous 3,5-bis(amide) pyridinium containing rotaxane. The rotaxane displays a strong preference for the halide anions over the larger, more basic oxoanions, although this is not as pronounced as was observed with the catenane analogue **1·PF$_6$**.[38]

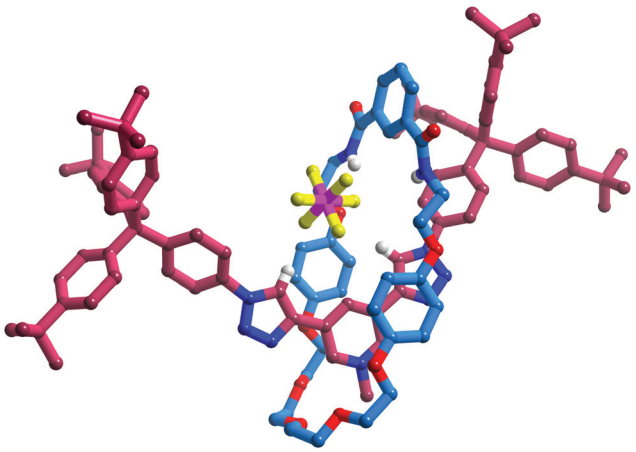

Fig. 2 Solid state structure of **7·PF$_6$**. Solvent molecules, and most hydrogen atoms are omitted for clarity.

This is perhaps unexpected, as amide based rotaxane host systems have typically exhibited a much higher degree of selectivity for halides over oxoanions than analogous catenanes, attributed to their more rigid nature.[39] Importantly, enhanced selectivity is however observed for the new triazole containing rotaxane host over catenane analogue **1·PF$_6$**[38] in discrimination between the halide anions. A tentative explanation for this can be postulated by considering the differing binding modes of the various anions: the halides bind inside the interlocked hosts' three-dimensional cavities[39] allowing the more rigid rotaxane to exhibit a degree of selectivity that is absent in the catenane. Conversely, the larger basic oxoanions associate on the exterior of the host,[40] and so are affected more by the strongest donor groups in the host, in this case the charged bis-triazole pyridinium motif, and less by the three-dimensional cavity. The aryl-substituted bis-triazole pyridinium

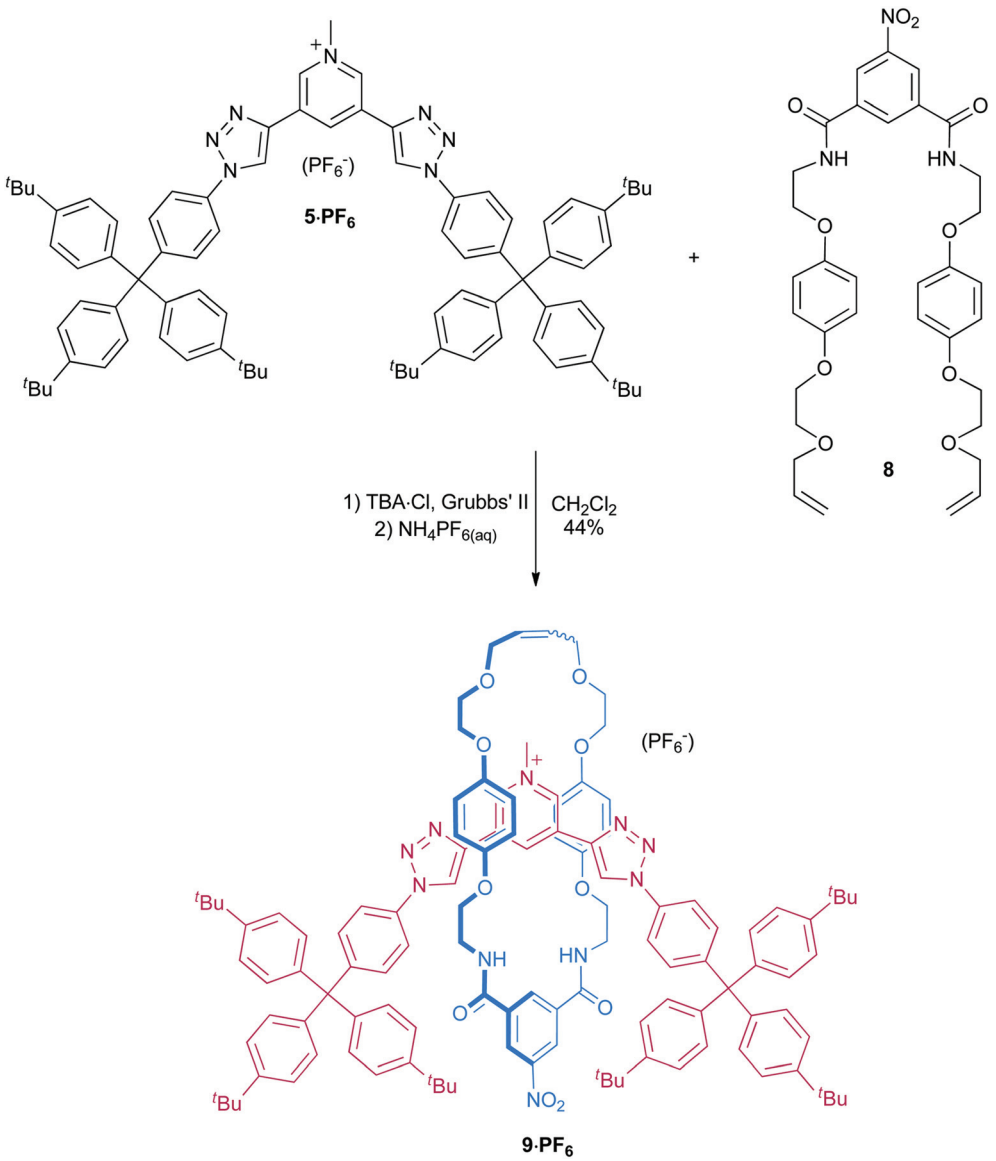

Scheme 3 Synthesis of rotaxane **9·PF$_6$**.

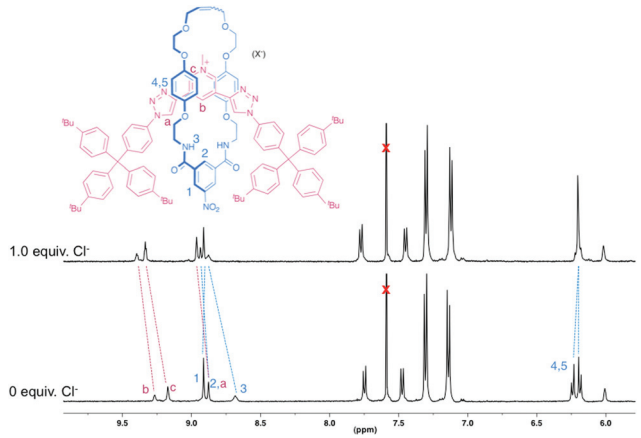

Fig. 3 Truncated ^{1}H NMR spectrum of **9·PF$_6$** upon addition of one equivalent of chloride anion (293 K, 1 : 1 $CDCl_3$–CD_3OD, 500 MHz).

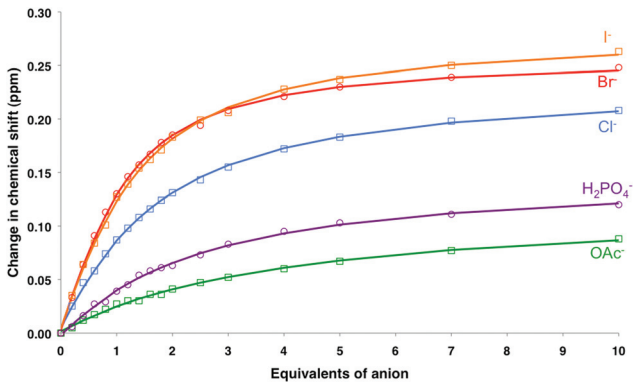

Fig. 4 Experimental titration data (points) and fitted binding isotherms (lines) for addition of anions to **9·PF$_6$** (293 K, 1 : 1 $CDCl_3$–CD_3OD, 500 MHz).

Table 1 Association constants, K_a (M^{-1}) for anions and pyridinium bis-triazole interlocked host systems[a]

Anion	Rotaxane **9·PF$_6$**	Catenane **1·PF$_6$**[38]
Cl^-	411(18)	679(20)
Br^-	936(40)	632(45)
I^-	640(29)	509(10)
$H_2PO_4^-$	186(9)	49(4)
OAc^-	137(3)	—[b]

[a] Anions added as TBA salts, estimated standard errors are given in parentheses. Association constants calculated using WINEQNMR2[48] (1 : 1 $CDCl_3$–CD_3OD, 293 K). [b] Movement of peaks too small to infer a binding event.

motif in the rotaxane is a more potent anion complexant than the alkyl-substituted motif in the catenane, and so stronger recognition of the oxoanions, and concomitant reduced selectivity results.

Small single crystals of **9·Cl** suitable for synchrotron X-ray structural analysis were obtained from the ^{1}H NMR titration experiment (Fig. 5). The chloride anion is bound within the rotaxane's host cavity with significant hydrogen bonds observed from both amide and both triazole groups, as well as

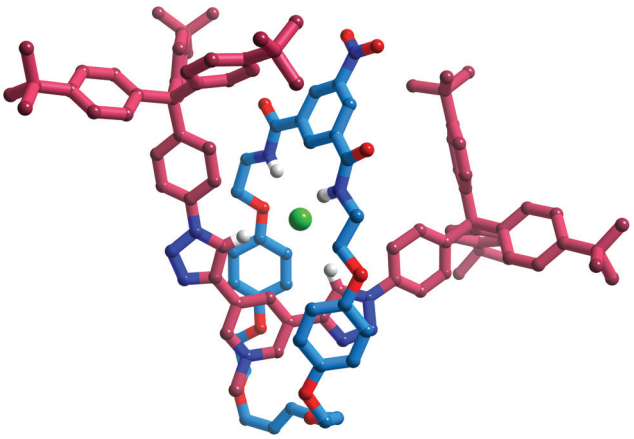

Fig. 5 Solid state structure of **9·Cl**. Minor position of ^{t}butyl disorder, and most hydrogen atoms omitted for clarity.

the axle component's *para*-pyridinium proton and the macrocycle's interior phenylene proton. Receptor···anion hydrogen bonds are significantly shorter in this structure than in the crystal structure of catenane **1·Cl**, although no pyridinium···hydroquinone aromatic donor–acceptor interactions are present in the solid state structure of the rotaxane, which were observed in the catenane crystal structure.

Conclusions

Two novel rotaxanes incorporating the bis-triazole pyridinium motif have been prepared. It was found that an amide condensation route gave relatively low yields of the interlocked product (20% crude yield, 11% isolated yield), while a chloride anion templated ring-closing metathesis strategy was significantly more successful (65% crude yield, 44% isolated yield). It is noteworthy that rotaxane **9·PF$_6$** displays an unusual preference for bromide over the other halide anions, and all halides are bound significantly more strongly than the larger more basic oxoanions. The selectivity preferences for the rotaxane are markedly different from the bis-triazole containing catenane **1·PF$_6$**,[38] which displays little preference between the halide anions, but a more pronounced selectivity for the halides over oxoanions.

Experimental

General remarks

TBTA,[49] tetraphenyl amine **3**,[42] bis-amine **6**,[46] and macrocycle precursor **8**[47] were prepared as previously described. 3,5-Diethynyl pyridine was prepared by deprotecting bis-(trimethylsilylethynyl)pyridine[50] using KOH in methanol.[51] Other chemicals are available commercially, and used as received. Where solvents are specified as "dry", they were purged with nitrogen and passed through an MBraun MPSP-800 column. NEt_3 was distilled from, and stored over KOH pellets. Water was deionised and microfiltered using a

Milli-Q Millipore machine. TBA salts, TBTA and $[Cu(CH_3CN)_4](PF_6)$ were stored in a vacuum dessicator. Chromatography was performed on silica gel (particle size: 40–63 μm) or preparative TLC plates (20 × 20 cm, silica thickness: 1 mm). Details of instrumentation, copies of NMR spectra, and details of titration protocols are given in the ESI.†

Azide-appended stopper 2

Aniline stopper **3**, (1.01 g, 2.00 mmol) was suspended in 9 : 1 ethanol–conc. $HCl_{(aq)}$ (500 mL), and the mixture gently warmed, causing all material to dissolve. It was cooled to 0 °C and sodium nitrite (0.276 g, 4.00 mmol) was added, followed by sodium azide (0.260 g, 4.00 mmol). The reaction was stirred under a nitrogen atmosphere for an hour at 0 °C, before being allowed to warm to room temperature overnight. The reaction was diluted with water (200 mL), and extracted with diethyl ether (2 × 200 mL). The combined organic fractions were washed with saturated aqueous sodium carbonate (2 × 150 mL) and brine (150 mL), dried ($MgSO_4$) and taken to dryness under reduced pressure. The resulting white powder was taken up in 1 : 1 petrol–dichloromethane and filtered through a short pad of silica, washing through with further 1 : 1 petrol–dichloromethane. Evaporation of the solvent gave pure **2** as a white powder. Yield: 0.876 g (83%).

^{1}H NMR ($CDCl_3$): 7.24 (d, ^3J = 8.6 Hz, 6H, H_{Ar}), 7.17 (d, ^3J = 8.8 Hz, 2H, H_{Ar}), 7.07 (d, ^3J = 8.6 Hz, 6H, H_{Ar}), 6.90 (d, ^3J = 8.8 Hz, 2H, H_{Ar}), 1.30 (s, 54H, $H_{t\mathrm{Bu}}$). ^{13}C NMR ($CDCl_3$): 148.7, 144.5, 143.8, 137.4, 132.7, 130.8, 124.3, 117.9, 63.4, 34.5, 31.5. HRMS (EI/FI): 529.3448, calc. for $[C_{37}H_{43}N_3]^+$ = 529.3457.

Pyridine bis-triazole axle 4

The azide **2** (0.233 g, 0.440 mmol) and 3,5-diethynylpyridine (0.025 g, 0.20 mmol) were dissolved in CH_2Cl_2 (25 mL). DIPEA (0.090 mL, 0.065 g, 0.50 mmol), TBTA (0.021 g, 0.040 mmol), and $[Cu(CH_3CN)_4](PF_6)$ (0.015 g, 0.040 mmol) were added and the resulting yellow solution stirred at room temperature under a nitrogen atmosphere for 5 days. The reaction mixture was taken to dryness under reduced pressure and purified by column chromatography (3% CH_3OH in $CHCl_3$) to give **4** as a white powder. Yield: 0.197 g (83%).

^{1}H NMR ($CDCl_3$): 9.13 (d, ^4J = 1.9 Hz, 2H, H_{py}), 8.76 (t, ^4J = 1.9 Hz, 1H, H_{py}) 8.34 (s, 2H, H_{trz}), 7.66–7.69 (m, 4H, H_{Ar}), 7.42–7.45 (m, 4H, H_{Ar}), 7.25–7.29 (m, 12H, H_{Ar}), 7.11–7.14 (m, 12H, H_{Ar}), 1.32 (s, 54H, $H_{t\mathrm{Bu}}$). ^{13}C NMR ($CDCl_3$): 149.1, 148.9, 146.8, 145.1, 143.4, 134.5, 132.8, 130.8, 130.1, 126.7, 124.5, 119.6, 118.6, 63.8, 34.5, 31.5. HRESI-MS (pos.): 1208.7231, calc. for $[C_{83}H_{91}N_7Na]^+$ = 1208.7228.

Pyridinium bis-triazole axle 5·PF_6

The neutral axle component **4** (0.297 g, 2.50 mmol) was dissolved in dry CH_2Cl_2 (20 mL) in a vial. CH_3I (0.37 mL, 0.85 g, 6.0 mmol) was added, and the vial sealed. It was stirred at room temperature for 7 days and then purified by column chromatography (2% CH_3OH in $CHCl_3$) to give the product as its iodide salt. It was suspended in 7 : 3 acetone–H_2O (100 mL) and stirred for 16 hours with PF_6^--loaded Amberlite® anion exchange beads. The suspension was separated from the beads by decanting, and the acetone removed under reduced pressure. The remaining aqueous suspension was extracted with CH_2Cl_2 (4 × 50 mL) and the combined organic fractions washed with $NH_4PF_{6(aq)}$ (2 × 75 mL) and H_2O (2 × 75 mL), and then dried ($MgSO_4$) to give **5**·PF_6 as an off-white powder. Yield: 0.211 g (63%).

^{1}H NMR ($CDCl_3$): 9.21 (t, ^4J = 1.2 Hz, 1H, H_{py}), 9.18 (d, ^4J = 1.2 Hz, 2H, H_{py}), 8.83 (s, 2H, H_{trz}), 7.63–7.68 (m, 4H, H_{Ar}), 7.39–7.44 (m, 4H, H_{Ar}), 7.23–7.29 (m, 12H, H_{Ar}), 7.10–7.15 (m, 12H, H_{Ar}), 4.48 (s, 3H, H_{CH3}), 1.30 (s, 54H, $H_{t\mathrm{Bu}}$). ^{13}C NMR (d_6-DMSO): 148.5, 148.1, 143.3, 141.3, 135.3, 134.3, 133.8, 131.9, 130.6, 129.9, 124.7, 122.8, 119.8, 63.3, 48.7, 34.1, 31.1. ^{19}F NMR (d_6-DMSO): −71.2 (d, $J_{P,F}$ = 711 Hz). ^{31}P NMR (d_6-DMSO): −144.3 (septet, $J_{P,F}$ = 711 Hz). HRESI-MS (pos.): 1200.7586, calc. for $[C_{84}H_{94}N_7]^+$ = 1200.7565.

Amide condensation rotaxane 7·PF_6

The axle component **5**·PF_6 (0.040 g, 0.030 mmol) was dissolved in dry CH_2Cl_2 (50 mL). NEt_3 (0.010 mL, 0.0076 g, 0.075 mmol) was added, followed by bis-amine **6** (0.014 g, 0.030 mmol) and isophthaloyl dichloride (0.0061 g, 0.030 mmol) in dry CH_2Cl_2 (2 mL). The reaction was stirred at room temperature under a nitrogen atmosphere for 2 hours, washed with $HCl_{(aq)}$ (10%, 2 × 30 mL), brine (30 mL), dried ($MgSO_4$), and taken to dryness under reduced pressure. Integration of the crude ^{1}H NMR spectrum suggested the rotaxane was formed in approximately 20% yield. The crude solid was purified by preparative TLC (3% CH_3OH in CH_2Cl_2), then taken up in CH_2Cl_2 (20 mL) and washed with $NH_4PF_{6(aq)}$ (0.1 M, 6 × 20 mL) and H_2O (2 × 20 mL). Drying thoroughly *in vacuo* gave 7·PF_6 as a white powder, which was shown by ^{1}H NMR spectroscopy to contain small amounts of impurities. Yield: 0.0062 g (11%). A pure sample was obtained by recrystallization from CH_3OH–$CHCl_3$ (4 : 1).

^{1}H NMR (1 : 1 $CDCl_3$–CD_3OD): 9.03 (s, 2H, H_{py}), 8.93 (s, 2H, H_{trz}), 8.68 (s, 1H, H_{py}), 8.51 (s, 1H, $H_{int.\ macro.\ Ar\ CH}$), 8.01–8.06 (m, 3H, $H_{ext.\ macro.\ Ar\ CH}$), 7.68 (d, J = 8.8 Hz, 4H, H_{Ar}), 7.43 (d, J = 8.8 Hz, 4H, H_{Ar}), 7.31–7.34 (m, 12H, H_{Ar}), 7.12–7.15 (m, 12H, H_{Ar}), 6.36 (d, J = 9.1 Hz, 4H, $H_{hydroquinone}$), 6.17 (d, J = 9.1 Hz, 4H, $H_{hydroquinone}$), 4.43 (s, 3H, H_{CH3}), 3.88 (t, J = 4.8 Hz, 4H, H_{CH2}), 3.82–3.84 (m, 4H, H_{CH2}), 3.73–3.75 (m, 4H, H_{CH2}), 3.64–3.71 (m, 8H, H_{CH2}), 3.51–3.53 (m, 4H, H_{CH2}), 1.30 (s, 54H, $H_{t\mathrm{Bu}}$). ^{19}F NMR ($CDCl_3$): −73.4 (d, $J_{P,F}$ = 711 Hz). HRESI-MS (pos.): 1911.0968, calc. for $[C_{122}H_{144}N_9O_{11}]^+$ = 1911.0980.

Clipping rotaxane 9·PF_6

The pyridinium bis-triazole axle component **5**·PF_6 (0.034 g, 0.025 mmol) was dissolved in dry CH_2Cl_2 (70 mL), and the solution reduced in volume to 20 mL under reduced pressure. The macrocycle precursor **8** (0.024 g, 0.038 mmol), TBA·Cl (0.0069 g, 0.025 mmol) and Grubbs' II catalyst (0.0024 g, 10% by weight) were added, and the mixture stirred at room temperature under a nitrogen atmosphere for 3 days. It was taken to dryness and purified by preparative TLC (2% CH_3OH

in CH_2Cl_2) to give a crude product containing a mixture of rotaxane and ring-closed macrocycle (accounting for the presence of macrocycle impurity, the yield at this point was estimated to be 65% on the basis of ^{1}H NMR analysis). This material was taken up in CH_2Cl_2 (20 mL), washed with $NH_4PF_{6(aq)}$ (0.1 M, 7 × 20 mL), and H_2O (3 × 20 mL) and taken to dryness. Recrystallization from CH_3OH–$CHCl_3$ (5 mL, ~4 : 1) gave pure **9·PF$_6$** as a pale yellow powder. Yield: 0.022 g (44%).

^{1}H NMR (1 : 1 $CDCl_3$–CD_3OD): 9.15 (s, 1H, H_{py}), 9.03 (s, 2H, H_{py}), 8.84–8.87 (m, 3H, $H_{int.\ macro.Ar\ CH}$, 2 × H_{trz}), 8.78 (s, 2H, $H_{ext.\ macro.\ Ar\ CH}$), 8.53 (br. s, 2H, H_{amide}), 7.70 (d, J = 8.8 Hz, 4H, H_{Ar}), 7.45 (d, J = 8.8 Hz, 4H, H_{Ar}), 7.28 (d, J = 8.6 Hz, 12H, H_{Ar}), 7.12 (d, J = 8.6 Hz, 12H, H_{Ar}), 6.14–6.27 (m, 8H, $H_{hydroquinone}$), 5.99 (br. s, 2H, H_{alkene}), 4.39 (s, 3H, H_{CH3}), 4.03–4.06 (m, 4H, H_{CH2}), 3.65–3.86 (m, 16H, H_{CH2}), 1.30 (s, 54H, H_{tBu}). ^{13}C NMR (1 : 1 $CDCl_3$–CD_3OD): 166.7, 153.5, 153.3, 150.2, 149.5, 149.3, 144.1, 141.7, 140.2, 137.0, 135.4, 134.6, 133.3, 132.5, 132.1, 131.3, 130.5, 126.1, 125.1, 122.4, 119.7, 115.5, 115.1, 78.5, 71.5, 69.9, 68.4, 67.3, 64.4, 40.8, 34.9, 31.7. ^{19}F NMR (1 : 1 $CDCl_3$–CD_3OD): −72.6 (d, $J_{P,F}$ = 712 Hz). ^{31}P NMR (1 : 1 $CDCl_3$–CD_3OD): −144.3 (septet, $J_{P,F}$ = 712 Hz). HRESI-MS (pos.): 1821.9881, calc. for $[C_{116}H_{129}N_{10}O_{10}]^+$ = 1821.9888.

X-ray crystallography

Crystals of **7·PF$_6$** and **9·Cl** were very small and weakly-diffracting. Therefore, single crystal X-ray diffraction data were collected on Beamline I19 of Diamond Lightsource[52] using synchrotron radiation (λ = 0.6889 and 1.1949 Å for **7·PF$_6$** and **9·Cl**, respectively). A Cryostream N2[53] open-flow cooling device was used to cool the samples to 100 K. Series of scans were performed in such a way as to collect a complete set of unique reflections to a maximum of 0.80 Å for **7·PF$_6$** and approximately 1.0 Å for **9·Cl**. Raw frame data (including data reduction, inter-frame scaling, unit cell refinement and absorption corrections) were processed using CrysAlisPro.[54] The structures were solved by charge-flipping methods using SUPERFLIP[55] and refined using full-matrix least-squares on F^2 within the CRYSTALS suite.[56] All non-hydrogen atoms were refined with anisotropic displacement parameters. Hydrogen atoms were generally visible in the difference map and were initially refined with restraints on bond lengths and angles, after which the positions were used as the basis for a riding model.[57] Crystals of **7·PF$_6$** were found to be twinned: an appropriate twin law was determined using the ROTAX package,[58] within the CRYSTALS suite.[56] The relative fraction of each twin component was refined. An area of diffuse electron density was present in the structure of **9·Cl**, believed to be a result of disordered solvent molecules. This could not be sensibly modelled, and so PLATON-SQUEEZE[59,60] was used to include this electron density in the refinement. Crystallographic data for the structures have been deposited with the Cambridge Crystallographic Data Centre. CCDC: 911205 and 911206.†

Acknowledgements

We thank Diamond Lightsource for an award of beamtime on Beamline I19. NGW thanks the Clarendon Fund, Trinity College Oxford, and the Vice-Chancellors' Fund for financial support.

Notes and references

1 H. Juwarker, J. M. Lenhardt, D. M. Pham and S. L. Craig, *Angew. Chem., Int. Ed.*, 2008, **47**, 3740–3743.
2 Y. Li and A. H. Flood, *Angew. Chem., Int. Ed.*, 2008, **47**, 2649–2652.
3 R. M. Meudtner and S. Hecht, *Angew. Chem., Int. Ed.*, 2008, **47**, 4926–4930.
4 Y. Li, M. Pink, J. A. Karty and A. H. Flood, *J. Am. Chem. Soc.*, 2008, **130**, 17293–17295.
5 Y. Li and A. H. Flood, *J. Am. Chem. Soc.*, 2008, **130**, 12111–12122.
6 Y. Hua and A. H. Flood, *J. Am. Chem. Soc.*, 2010, **132**, 12838–12840.
7 S. Lee, Y. Hua and H. P. A. H. Flood, *Org. Lett.*, 2010, **12**, 2100–2102.
8 Y. Hua, R. O. Ramabhadran, E. O. Uduehi, J. A. Karty, K. Raghavachari and A. H. Flood, *Chem.–Eur. J.*, 2011, **17**, 312–321.
9 R. O. Ramabhadran, Y. Hua, Y. Li, A. H. Flood and K. Raghavachari, *Chem.–Eur. J.*, 2011, **17**, 9123–9129.
10 K. McDonald, R. O. Ramabhadran, S. Lee, K. Raghavachari and A. H. Flood, *Org. Lett.*, 2011, **13**, 6260–6263.
11 Y. Hua, R. O. Ramabhadran, J. A. Karty, K. Raghavachari and A. H. Flood, *Chem. Commun.*, 2011, **47**, 5979–5981.
12 H. Juwarker, J. M. Lenhardt, J. C. Castillo, E. Zhao, S. Krishnamurthy, R. M. Jamiolkowski, K.-H. Kim and S. L. Craig, *J. Org. Chem.*, 2009, **74**, 8924–8934.
13 Y. Wang, F. Bie and H. Jiang, *Org. Lett.*, 2010, **12**, 3630–3633.
14 Y. Wang, J. Xiang and H. Jiang, *Chem.–Eur. J.*, 2011, **17**, 613–619.
15 V. Haridas, S. Sahu and P. Venugopalan, *Tetrahedron*, 2011, **67**, 727–733.
16 M. R. Krause, R. Goddard and S. Kubik, *J. Org. Chem.*, 2011, **76**, 7084–7095.
17 C.-H. Lee, S. Lee, H. Yoon and W.-D. Jang, *Chem.–Eur. J.*, 2011, **17**, 13898–13903.
18 Q.-Y. Cao, T. Pradhan, S. Kim and J. S. Kim, *Org. Lett.*, 2011, **13**, 4386–4389.
19 Y.-H. Lau, P. J. Rutledge, M. Watkinson and M. H. Todd, *Chem. Soc. Rev.*, 2011, **40**, 2848–2866.
20 F. García, M. R. Torres, E. Matesanz and L. Sánchez, *Chem. Commun.*, 2011, **47**, 5016–5018.
21 L. C. Gilday, N. G. White and P. D. Beer, *Dalton Trans.*, 2012, **41**, 7092–7097.
22 G. Yu, Z. Zhang, C. Han, M. Xue, Q. Zhou and F. Huang, *Chem. Commun.*, 2012, **48**, 2958–2960.

23 N. G. White and P. D. Beer, *Supramol. Chem.*, 2012, **24**, 473–480.
24 S. C. Picot, B. R. Mullaney and P. D. Beer, *Chem.–Eur. J.*, 2012, **18**, 3620–3626.
25 Y.-J. Li, L. Xu, W.-L. Yang, H.-B. Liu, S.-W. Lai, C.-M. Che and Y.-L. Li, *Chem.–Eur. J.*, 2012, **18**, 4782–4790.
26 L. Xu, Y. Li, Y. Yu, T. Liu, S. Cheng, H. Liu and Y. Li, *Org. Biomol. Chem.*, 2012, **10**, 4375–4380.
27 Q.-Y. Cao, T. Pradhan, M. H. Lee, D. H. Choi and J. S. Kim, *Tetrahedron Lett.*, 2012, **53**, 4917–4920.
28 M. Caricato, A. Olmo, C. Gargiulli, G. Gattuso and D. Pasini, *Tetrahedron*, 2012, **68**, 7861–7866.
29 V. V. Rostovtsev, L. G. Green, V. V. Fokin and K. B. Sharpless, *Angew. Chem., Int. Ed.*, 2002, **41**, 2596–2599.
30 C. W. Tornøe, C. Christensen and M. Meldal, *J. Org. Chem.*, 2002, **67**, 3057–3064.
31 A. Fahrenbach and J. F. Stoddart, *Chem.–Asian J.*, 2011, **6**, 2660–2669.
32 K. D. Hänni and D. A. Leigh, *Chem. Soc. Rev.*, 2010, **39**, 1240–1251.
33 A. Joosten, Y. Trolez, J.-P. Collin, V. Heitz and J.-P. Sauvage, *J. Am. Chem. Soc.*, 2012, **134**, 1802–1809.
34 H. Lahlali, K. Jobe, M. Watkinson and S. M. Goldup, *Angew. Chem., Int. Ed.*, 2011, **50**, 4151–4155.
35 Y. Yamada, M. Okamoto, K. Furukawa, T. Kato and K. Tanaka, *Angew. Chem., Int. Ed.*, 2012, **51**, 709–713.
36 An anion binding indolocarbazole catenane that contains triazole groups has also been reported, although the key anion recognition motif appears to be the indolocarbazole unit (Y. Zhao, Y. Li, Y. Li, H. Zheng, X. Yin and H. Liu, *Chem. Commun.*, 2010, **46**, 5698–5700).
37 H. Zheng, W. Zhou, J. Lv, X. Yin, Y. Li, H. Liu and Y. Li, *Chem.–Eur. J.*, 2009, **15**, 13253–13262.
38 N. G. White and P. D. Beer, *Chem. Commun.*, 2012, **48**, 8499–8501.
39 M. D. Lankshear and P. D. Beer, *Acc. Chem. Res.*, 2007, **40**, 657–668.
40 L. M. Hancock, L. C. Gilday, S. Carvalho, P. J. Costa, V. Félix, C. J. Serpell, N. L. Kilah and P. D. Beer, *Chem.–Eur. J.*, 2010, **16**, 13082–13094.
41 J. A. Wisner, P. D. Beer, M. G. B. Drew and M. R. Sambrook, *J. Am. Chem. Soc.*, 2002, **124**, 12469–12476.
42 H. W. Gibson, S.-H. Lee, P. T. Engen, P. Lecavalier, J. Sze, Y. X. Shen and M. Bheda, *J. Org. Chem.*, 1993, **58**, 3748–3756.
43 E. Bosch and C. L. Barnes, *Organometallics*, 2000, **19**, 5522–5524.
44 L. M. Hancock and P. D. Beer, *Chem.–Eur. J.*, 2009, **15**, 42–44.
45 The hexafluorophosphate salt of the axle component was used due to the very low solubility of **5·Cl** in organic solvents. This is expected to have only a very minor effect on rotaxane formation as chloride anion is produced during amide condensation.
46 K.-Y. Ng, V. Félix, S. M. Santos, N. H. Rees and P. D. Beer, *Chem. Commun.*, 2008, 1281–1283.
47 M. R. Sambrook, P. D. Beer, M. D. Lankshear, R. F. Ludlow and J. A. Wisner, *Org. Biomol. Chem.*, 2006, **4**, 1529–1538.
48 M. J. Hynes, *J. Chem. Soc., Dalton Trans.*, 1993, 311–312.
49 B.-Y. Lee, S. R. Park, H. B. Jeon and K. S. Kim, *Tetrahedron Lett.*, 2006, **47**, 5105–5109.
50 H. Goto, J. M. Heemstra, D. J. Hill and J. S. Moore, *Org. Lett.*, 2004, **6**, 889–892.
51 T. X. Neenan and G. M. Whitesides, *J. Org. Chem.*, 1988, **53**, 2489–2496.
52 H. Nowell, S. A. Barnett, K. E. Christensen, S. J. Teat and D. R. Allan, *J. Synchrotron Radiat.*, 2012, **19**, 435–441.
53 J. Cosier and A. M. Glazer, *J. Appl. Crystallogr.*, 1986, **19**, 105.
54 *CrysAlisPro*, Oxford Diffraction, 2011.
55 L. Palatinus and G. Chapuis, *J. Appl. Crystallogr.*, 2007, **40**, 786.
56 P. W. Betteridge, J. R. Carruthers, R. I. Cooper, K. Prout and D. J. Watkin, *J. Appl. Crystallogr.*, 2003, **36**, 1487.
57 R. I. Cooper, A. L. Thompson and D. J. Watkin, *J. Appl. Crystallogr.*, 2010, **43**, 1100.
58 R. I. Cooper, R. O. Gould, S. Parsons and D. J. Watkin, *J. Appl. Crystallogr.*, 2002, **35**, 168–174.
59 A. Spek, *J. Appl. Crystallogr.*, 2003, **36**, 7–13.
60 P. S. van der Sluis and A. L. Spek, *Acta Crystallogr., Sect. A: Fundam. Crystallogr.*, 1990, **46**, 194–201.